Agricultural and Forest Meteorology 351 (2024) 110016

Contents lists available at ScienceDirect

Agricultural and Forest Meteorology

journal homepage: www.elsevier.com/locate/agrformet

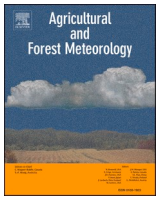

Wildfire impacts on the carbon budget of a managed Nordic boreal forest

Julia Kelly [a,*], Natascha Kljun [a], Zhanzhang Cai [b], Stefan H. Doerr [c], Claudio D'Onofrio [b], Thomas Holst [b], Irene Lehner [a], Anders Lindroth [b], Shangharsha Thapa [b], Patrik Vestin [b], Cristina Santín [d,e]

[a] Centre for Environmental and Climate Science, Lund University, Sweden
[b] Department of Physical Geography and Ecosystem Science, Lund University, Sweden
[c] Geography Department, Swansea University, UK
[d] Research Institute of Biodiversity (IMIB), Spanish National Research Council-University of Oviedo, Spain
[e] Biosciences Department, Swansea University, UK

ARTICLE INFO

Keywords:
Eddy covariance
Net ecosystem exchange
Forest fire
Salvage-logging
Forest management
Fennoscandia

ABSTRACT

Wildfire is one of the most important disturbances affecting boreal forests. Most previous research on boreal forest fires has occurred in North American forests which have different fire regimes, tree species and are less intensively managed than their Eurasian counterparts. Recent extreme fire years have highlighted the vulnerability of the Nordic boreal forest to climatic shifts that are increasing forest fire frequency and severity. The Ljusdal fire (2018) was one of the largest wildfires in recorded history in Sweden. We established eddy covariance flux towers to track the impacts of this fire on the carbon balance of two *Pinus sylvestris* sites subject to different fire severities and forest management strategies 1–4 years post-fire. The 'SLM' site was a mature stand that experienced low-severity fire (trees survived) followed by salvage-logging and reseeding, whilst the 'HY' site was 10 years old when it experienced high-severity fire (all trees killed) then was replanted with seedlings. During the study period, both sites were net carbon sources at the annual scale. It took up to 4 years after the fire until the first day of net CO_2 uptake was recorded at each site. We estimated that it will take 13 years (8, 21; mean ± 95 % confidence intervals) after the fire until the sites reach a neutral annual carbon balance. It will take up to 32 years (19, 53) at HY and 46 years (31, 70) at SLM to offset the carbon lost during and after the fire and salvage-logging. In addition, our measurements showed that more carbon was emitted in the first 4 years after the fire compared to the carbon lost from combustion during the fire. Quantifying carbon fluxes during the initial years after fire is therefore crucial for estimating the net impact of wildfire on the carbon budget of boreal forests.

1. Introduction

Boreal forests store vast amounts of carbon but it is uncertain whether they will remain carbon sinks as disturbances become more frequent with climate change and increasing resource exploitation (Anderegg et al., 2022). Wildfire is one of the most important disturbances affecting boreal forests and leads to large immediate losses of carbon (Bond-Lamberty et al., 2007). The net effect of fire on the forest carbon balance ultimately depends on how fast the forest recovers before the next disturbance. In some parts of the boreal region, the frequency of wildfires in the last few decades is already higher than at any other period during the last 10 000 years, threatening not only ongoing carbon sequestration but also long-term carbon stores (Feurdean et al., 2020; Kelly et al., 2013; Walker et al., 2019).

The immediate post-fire years are critical for setting the recovery trajectory of burnt forests because this is when the most dramatic changes occur in the carbon exchange between the forest and the atmosphere (Amiro, 2001). The net carbon dioxide (CO_2) balance of a forest stand can be defined as the Net Ecosystem Exchange (NEE), which is the difference between CO_2 uptake by photosynthesis (Gross Primary Productivity, GPP) and CO_2 emissions from vegetation and soil respiration (together known as Ecosystem Respiration, ER). Boreal forests in North America tend to become a net source of carbon after fire because the typical stand-replacing fires cause ER to easily outweigh the GPP of any remaining vegetation (Goulden et al., 2011). Previous estimates from Canada suggest it can take at least a decade after fire for a forest to become a net CO_2 sink at the annual scale, although daytime net uptake of CO_2 occurs earlier (Amiro et al., 2003; Goulden et al., 2011). The

* Corresponding author.
E-mail address: julia.kelly@cec.lu.se (J. Kelly).

https://doi.org/10.1016/j.agrformet.2024.110016
Received 19 October 2023; Received in revised form 10 April 2024; Accepted 13 April 2024
Available online 22 April 2024

emission of CO_2 in post-fire forest stands can add up to a significant proportion of the carbon emitted during the fire itself, emphasizing the importance of measuring carbon after a fire (Ueyama et al., 2019). In addition, fire changes light availability and soil temperature, moisture retention and chemistry, which feedback to influence the recovery of vegetation and soil microbiota (Bansal et al., 2014; Gustafsson et al., 2020). As a result, ecosystem carbon fluxes are affected for decades following fire (Dooley and Treseder, 2012; Mack et al., 2021).

Flux towers provide high frequency measurements of NEE that can be partitioned into ER and GPP to examine how the ecosystem CO_2 balance changes over time since fire and what factors drive these changes. Although there are previous flux tower studies in burnt boreal forests, several knowledge gaps remain. Firstly, most work has been carried out in North American boreal forests, which have different tree species and fire regimes to those in Eurasia (De Groot et al., 2013). In Eurasian forests, low-severity surface fires are the norm, in contrast to the stand-replacing crown fires in North America. In addition, most studies have used chronosequences (e.g. Amiro et al., 2006; Goulden et al., 2011; Litvak et al., 2003; Mkhabela et al., 2009), with very few measuring NEE over multiple years at the same site, especially in the period immediately after fire (Ueyama et al., 2019). Lastly, to the authors' knowledge there are no flux tower studies that explicitly consider how boreal forests are managed after fire, even though these decisions could have a large influence on the CO_2 exchange of the burnt forest.

Over half of the boreal forest area is managed, although management intensity varies widely across the region (Gauthier et al., 2015). In the Nordic countries, >70 % of forest area is intensively managed for timber production and as a result, fire suppression has been highly successful (Högberg et al., 2021; Trivino et al., 2022). Nevertheless, in 2018 Sweden experienced an unprecedented number of wildfires during a severe and long-lasting drought. This extreme fire season overwhelmed firefighting resources and highlighted the vulnerability of the region to fire, especially as hot and dry extremes are predicted to become more common (IPCC, 2023). In forests managed for commercial production, owners must often make rapid decisions after fire of whether to salvage-log, how to replant and with what species. Our lack of understanding of the effects of these choices on the forest carbon balance hampers sustainable decision-making.

Shortly after the extreme 2018 fire season, we established two eddy-covariance flux towers in Scots pine (*Pinus sylvestris*) stands affected by the Ljusdal fire in Sweden, which was the largest area burnt that year. The two sites contrast in terms of fire severity, age of the trees at the time of the fire and post-fire forest management. Our estimates of NEE, ER and GPP cover the first four growing seasons after the fire and contribute to filling the data gap in CO_2 flux measurements in the early post-fire years for Eurasian fires. We track how post-fire management decisions have shaped the recovery of vegetation at the sites and their carbon sink capacity.

2. Methods

2.1. Study area

Our two study sites are located within the area burnt by the Ljusdal fire in central Sweden (61°56′N, 15°28′E; Fig. 1a). The area is dominated by managed *Pinus sylvestris* forests with a lichen and shrub understory.

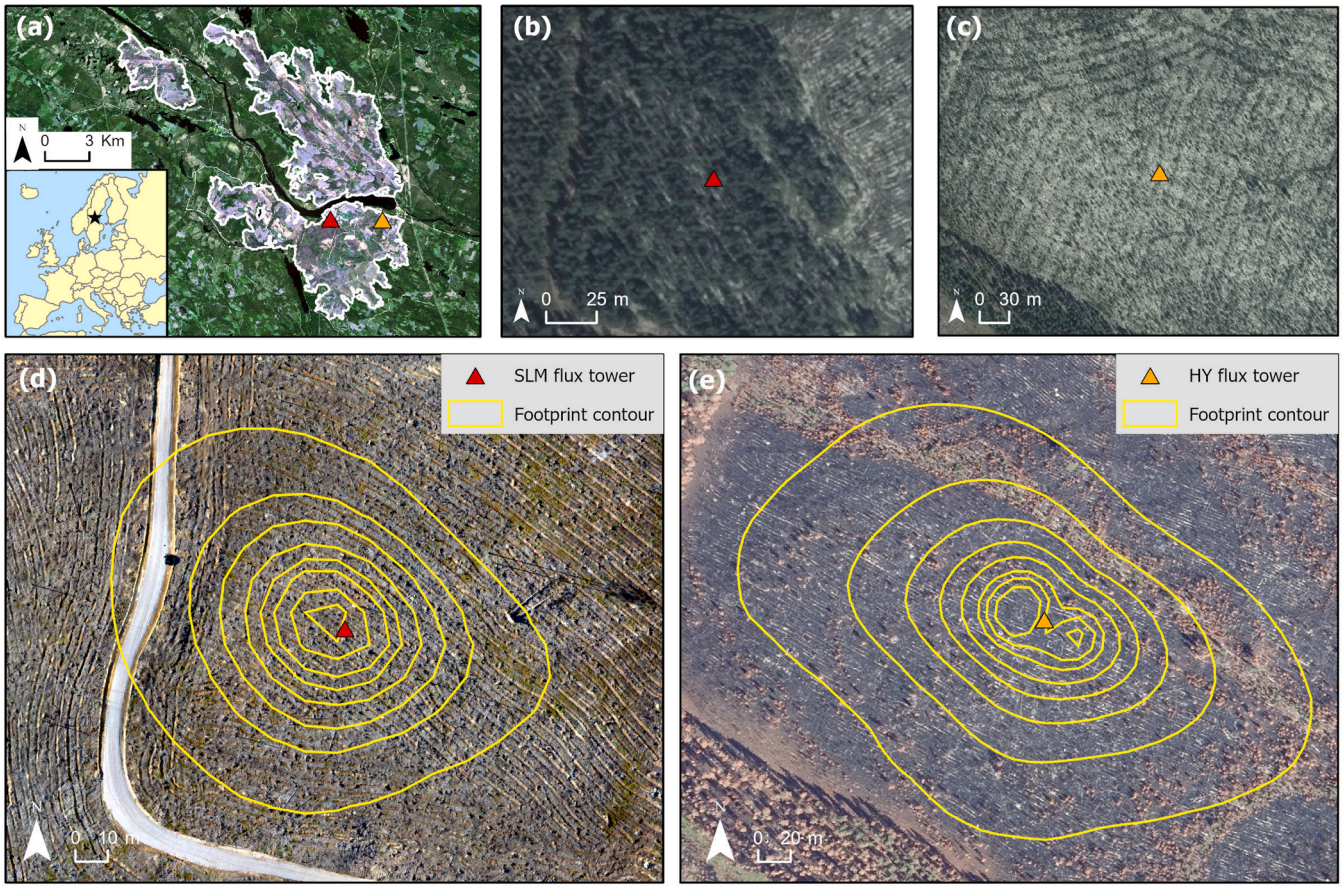

Fig. 1. a) Location of the SLM (Salvage-logged Low-severity Mature site; red triangle) and HY (High-severity Young site; orange triangle) flux towers within the Ljusdal fire area with inset map showing site location (black star) within Europe. b) and c) are aerial photos showing SLM and HY sites in 2017 before the fire. d) and e) are drone orthomosaics showing SLM in 2020 and HY in 2018 after the fire with flux tower location and footprint outline (10–80 % contours of FFP model; (Kljun et al., 2015). Data sources: EuroGeographics, ESA, Lantmäteriet, Skogsstyrelsen.

The fire occurred in July 2018 and was ignited by lightning strikes that hit forests already suffering from a long and severe drought. The fire burned 8995 ha, making it the second largest in Sweden within the last century. Fire severity varied across the burnt area with complete tree mortality in some areas (which we define as high-severity fire) and complete tree survival with bark scorching in others (which we define as low-severity fire). Our two study sites are located within 3 km of each other and therefore experienced the same weather conditions. The average annual air temperature between 2019 and 2022 when our measurements were conducted was 3.8 °C and the average annual precipitation was 652 mm (Ytterhogdal, SMHI 2023). For more details about the study area and fire please see Kelly et al. (2021).

In August 2019, one year after the fire, we installed an eddy covariance (EC) flux tower system at a young *Pinus sylvestris* forest that was affected by high-severity fire in which all trees died (in the following called HY, High-severity Young; Table 1). All vegetation was consumed during the fire, leaving only a thin forest floor layer at the site. The dead trees were left standing and in the summer of 2020 the site was replanted with nursery seedlings of *Pinus sylvestris* without any ground preparation being undertaken (Fig. 2d). Since the fire, wind erosion has exposed more and more of the white sandy mineral layer and many of the dead trees have fallen (Fig. 2b, d).

In June 2020, two years after the fire, we installed a second EC flux tower system at a mature *Pinus sylvestris* site which was affected by low-severity fire, i.e. the trees survived but the forest floor layer was consumed, (in the following called SLM, Salvage-logged Low-severity Mature; Table 1, Fig. 2a, c). The site was salvage-logged in the winter following the fire. Only the stumps and branches were left at the site. Soil scarification was performed, which created furrows of exposed loamy mineral soil interspersed with ridges of undisturbed burnt organic soil. After the scarification, seeds of *Pinus sylvestris* were spread across the site. We note that the forest owners were responsible for deciding which post-fire management practices were implemented at each site and we could not influence this decision.

2.2. Biometeorological measurements

At both sites, air temperature and humidity were measured at 2 m height with a HygroVUE10 (Campbell Scientific Inc., Logan, Utah, USA). Incoming and reflected photosynthetically active radiation (PAR) were measured with full-spectrum Quantum sensors (two downward facing sensors at HY and one at SLM; SQ-500-SS, Apogee Instruments, Logan, Utah, USA). A four-component net radiometer was also installed on both flux towers (SLM: SN-500, Apogee Instruments, Logan, Utah, USA; HY: CNR4, Kipp & Zonen, Delft, The Netherlands). At HY, precipitation was measured during snow-free periods using a rain gauge (ARG 314, Environmental Measurements Ltd., North Shields, United Kingdom) and gapfilled with national monitoring station data. At both sites soil temperature and volumetric soil water content were measured at three locations and two depths near the flux tower (7.5 cm and 15 cm; CS655, Campbell Scientific Inc., Logan, Utah, USA) and one soil temperature profile was also installed (3 cm, 7.5 cm and 15 cm depths, 107 temperature probes, Campbell Scientific Inc., Logan, Utah, USA). Soil heat flux was measured at 16 cm depth using one plate at HY and two plates at SLM (in disturbed mineral soil and below the undisturbed burnt organic layer; HFP01, Hukseflux Thermal Sensors, Delft, The Netherlands). The soil heat flux data was corrected to account for heat stored in the soil above the plates following Meyers (2004).

To compare the weather at our sites during the study period (2019–2022) with the long-term average, we used air temperature and precipitation data from the national monitoring station Ytterhogdal (263 m a.s.l, 40 km northwest of our sites, SMHI, 2023).

To track vegetation regrowth at the sites, we performed vegetation surveys in July 2020–2022. Percentage cover was visually estimated for all species within a 25 cm x 25 cm quadrat at 12 locations along 2 transects at each site. We also measured the height of all *Pinus sylvestris* seedlings within 4 circular plots of 3 m radius at the ends of the vegetation survey transects.

Table 1
Site characteristics. The forest floor refers to the soil organic layer and litter layer.

	HY	SLM
Coordinates	61.94°N, 15.48°E	61.94°N, 15.43°E
Altitude (m a.s.l.)	229	234
Fire severity	High	Low
Post-fire management	Dead trees left standing, pine seedlings replanted in summer 2020	Surviving trees salvage-logged, soil scarification and pine seed spreading in winter 2018/2019
Tree age in 2018 (years)	10	54
Forest floor thickness after fire (cm)	1.2	0–2.6
Charred forest floor thickness (cm)	0.8	0–1.1

2.3. Eddy covariance measurements

At HY, an LI-7500 gas analyser (LI-COR Environmental GmbH, Bad Homburg, Germany) and uSonic-3 Omni sonic anemometer (METEK GmbH, Elmshorn, Germany) were installed in 2019 at 5.45 m height. At SLM, an EC155 gas analyser with a CSAT3A sonic anemometer (both Campbell Scientific Inc., Logan, Utah, USA) were installed in 2020 at 2.15 m height (Table S1). When the sites were first established, they were powered by solar panels and batteries and thus no data was collected during the dark winter months (~November-March). In late 2021, SLM was connected to mainline power and could provide year-round data. The flux data and ancillary biometeorological measurements were processed in Eddy Pro (v.7.0.9, LI-COR Environmental GmbH, Bad Homburg, Germany). More details on the relevant corrections and filtering can be found in the Supplementary Information. The filtering resulted in between 28 and 35 % of the original 30 min periods of CO_2 data being discarded per year for SLM and 54–60 % for HY.

We used the REddyProc R package (Wutzler et al., 2018) to remove periods with low friction velocity (u_*), perform gapfilling and flux partitioning. The u_*-threshold was estimated for each year and site separately and varied between 0.06–0.11 ms^{-1}, leading to the removal of $\leq$20 % and $\leq$2 % of the CO_2 flux data at SLM and HY respectively. Net Ecosystem Exchange (NEE) was partitioned into Gross Primary Productivity (GPP) and Ecosystem Respiration (ER) using the daytime method and soil temperature (7.5 cm depth; Lasslop et al., 2010). We used the daytime method because there were very few dark night hours during the main growing season at the high latitude location of our sites. Note that in the daytime method, both GPP and ER are modelled estimates and therefore do not sum up exactly to NEE (Lasslop et al., 2010; Wutzler et al., 2018). We estimated the uncertainty (expressed as standard deviation) in the growing season sums of NEE, GPP and ER due to u* filtering and gapfilling, see the Supplementary Information and Tables S2-S4 therein. The combined uncertainty was between 2.5–18.0 g C m^{-2} growing season^{-1}, depending on the site and year, corresponding to 2–11 % of the growing season flux sum.

NEE data is presented using the micrometeorological sign convention of negative NEE as uptake of CO_2 and positive NEE as CO_2 emission from the ecosystem. The growing season energy balance closure was between 86 and 112 % at HY and 95–104 % at SLM based on daily mean soil, sensible and latent heat fluxes and net radiation between May and October. In our discussion of the EC data and other results, we define the 'growing season' as May 1 to October 31, (based on mean daily soil temperature >0 °C, Jarvis and Linder, 2000) and 'peak growing season' as June 1 to August 31, when the vegetation is most active at our sites.

The footprint climatology for both sites was calculated using the Flux

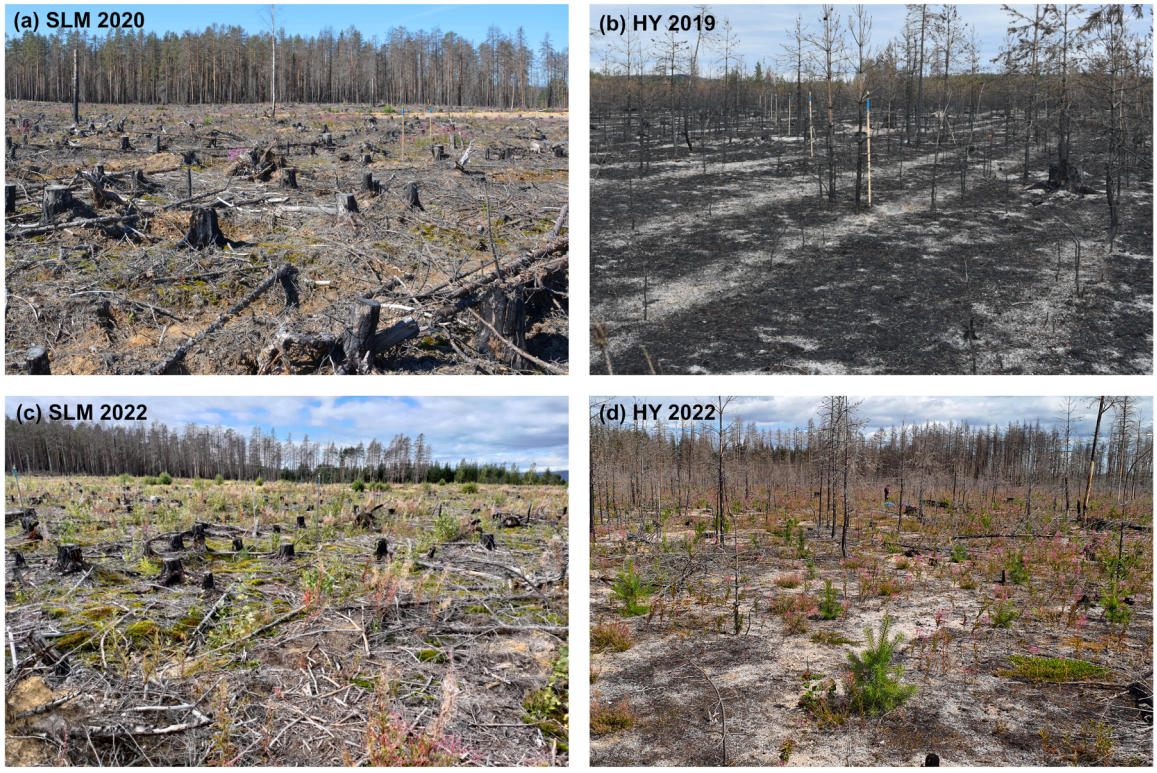

Fig. 2. Photos showing vegetation recovery at the sites since the fire a) in 2020 at SLM (Salvage-Logged Low-severity Mature), b) in 2019 at HY (High-severity Young), c) SLM in 2022, d) HY in 2022.

Footprint Prediction (FFP) model of Kljun et al. (2015) with the quality-controlled and filtered 30-min resolution EC data for all available years as input. The roughness length was estimated following Graf (2014).

2.4. Direct C loss from the fire and salvage-logging

We estimated the amount of C lost during the fire to compare with our EC measurements of C lost post-fire. At HY, the tree stems, branches and root biomass were not fully combusted and remained on site after the fire (see Fig. 2b, d). Hence the main tree-related C loss at HY was from the burnt needles and small twigs. Using allometric equations for Swedish *Pinus sylvestris* from Marklund (1988), we calculated a dry biomass of 0.4 kg per tree for needles and fine twigs, which upscaled to a loss of 0.0197 kg C m^{-2} at the site scale (based on a dry biomass C content of 50 % (Houghton et al., 2009) and a density of 984 trees ha^{-1} at HY). To calculate the loss of forest floor C due to combustion, and considering pre-fire measurements at the same site were not available, we measured the C in the forest floor in an unburnt young *Pinus sylvestris* site of similar age (within 2 km of HY), following the same protocol as in Kelly et al. (2021). The C stocks in the forest floor at the unburnt site were 0.965 kg C m^{-2} compared to 0.501 kg C m^{-2} at HY which gives a 0.464 kg C m^{-2} loss from the consumption of the forest floor during the fire. We considered the C lost from the shrub layer or small seedlings that were growing at the unburnt young site as negligible, as Granath et al. (2021) showed that the shrub layer only accounted for ~2 % of the total forest C loss found after another Swedish forest fire. Visual inspection at HY one year after the fire also did not reveal evidence of an abundant shrub cover before the fire.

At SLM, the only C loss during the fire came from the consumption of the forest floor layer, since the trees survived the fire (only bark scorched) and the tree stems were removed during the salvage-logging after the fire. We therefore used the value of 0.43 kg C m^{-2} lost from the forest floor estimated for a nearby (2.5 km), very similar, low-severity fire site in the Ljusdal fire area ('LM' site in Kelly et al., 2021). To calculate the amount of C removed from the ecosystem as a result of the salvage-logging, we used data on the timber volume (112 m^3 ha^{-1}) provided by the forest owner and an average wood density of 398 kg m^{-3} for *Pinus sylvestris* (Wilhelmsson et al., 2002), of which 50 % was C, giving a total C loss of 2.2 kg C m^{-2}. The C contained in the tree branches and needles was not included in our estimate of C loss because they were not removed from the site during the salvage-logging.

2.5. Carbon balance recovery after fire

To estimate the duration for NEE to recover after the fire, we modelled annual NEE over time since the fire using a model developed by Coursolle et al. (2012) for Canadian boreal forests recovering from logging or wildfire, where NEP = a*exp(b*stand age) + c*exp(d*stand age). The model was originally based on Net Ecosystem Productivity (NEP) but we present the results as NEE (i.e. NEE = -NEP). In this study, we fit the model separately to annual NEE estimates from HY and SLM, combined with NEE from 31 *Pinus sylvestris* stands in northern Sweden between 5 and 185 years old (Peichl et al., 2022a, 2022b), and an average annual NEE estimate for a 100 year old *Pinus sylvestris* stand also in northern Sweden (Rosinedalsheden; (Chi et al., 2021). It is important to note that the NEE data from Peichl et al. (2022a) and Chi et al. (2021) are from unburnt, harvested stands. To transform our growing season NEE measurements to annual NEE sums for use in the model, we added 13 % extra C emission, which is the proportion of C emitted during the dormant season based on data from SLM in 2022. See the Supplementary Information for information on the model parameters.

2.6. Spectral data

To track vegetation regrowth, a set of spectral sensors (SRS-NDVI, Decagon Devices, Pullman, Washington, USA) with red and NIR (near infrared) bands were installed in 2019 at HY. In 2020, the same sensors

were installed at SLM with an additional downward-facing sensor to better capture the spatial variability in vegetation regrowth. The data were processed to create daily means of EVI2 (2-band Enhanced Vegetation Index; (Jiang et al., 2008) following the SITES (2022) protocol. We refer to this in-situ data as $EVI2_{is}$.

To capture a timeline of vegetation greenness before and after the fire (2017–2022) we used Sentinel-2 data (S2, 10 m resolution) to calculate EVI2 ($EVI2_{S2}$) across the flux tower footprint area (up to the 80 % contour, applying footprint weighting). Using only cloud-free pixels, the data were gapfilled and smoothed pixel-wise to create daily time series using a spline in TIMESAT4 (CLMS, 2023; Jönsson and Eklundh, 2004). The data from our two burnt sites were compared to $EVI2_{S2}$ extracted for a nearby unburnt mature *Pinus sylvestris* site (henceforth referred to as 'UM', cf. Kelly et al. (2021), which had similar weather and soils as the HY and SLM sites. We also used MODIS 8-day composites (MOD09Q1, v.6.1, 250 m resolution) to extend the pre-fire EVI2 ($EVI2_{mod}$) timeseries to 2014. We could not produce a MODIS time series for the UM site because it was too small relative to the MODIS pixel size.

3. Results

3.1. Weather conditions 2019–2022

During the study period, growing season weather was within the range of variability experienced over the last 20 years (Fig. 3a, b). At the annual scale, 2019 was notably wetter than any other year during the measurement period (Fig. 3a, d). In addition, 2020 sticks out for being the warmest year of the last two decades (Fig. 3a), with very mild air temperatures during the start and end of the year (Fig. 3c).

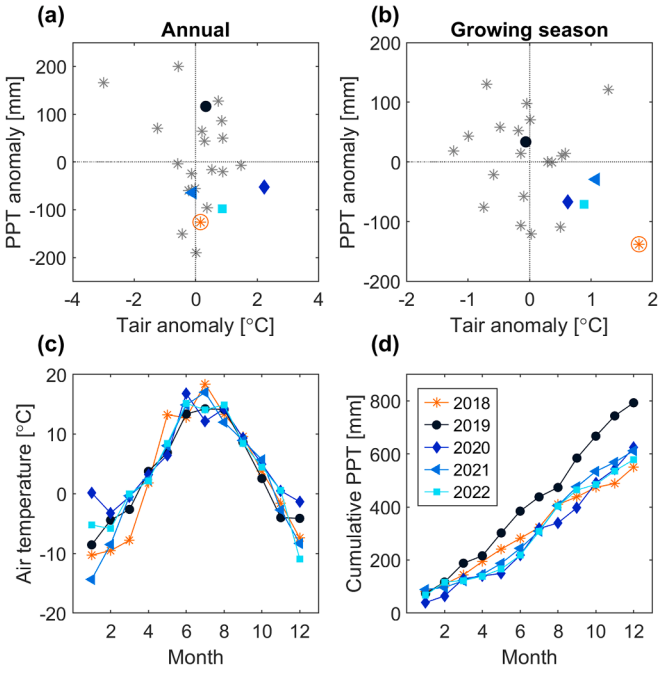

Fig. 3. (a) Annual and (b) growing season (1 May - 31 October) air temperature (Tair) versus precipitation (PPT) anomalies for 1999–2017 (grey asterisks) and study period 2019–2022 (coloured symbols). The circled orange asterisk highlights 2018, the year of the fire. (c) Monthly mean air temperature during the fire year and study period. (d) Cumulative monthly precipitation during the fire year and study period. All data are from the nearest national monitoring station (Ytterhogdal, 264 m a.s.l.; SMHI 2023).

3.2. SLM site

3.2.1. Soil conditions

At the SLM site, mean growing season soil temperature (±1σ) at 7.5 cm depth was 12.1 ± 0.5 °C and usually remained <20 °C even during the hottest periods (Fig. 4a). In the winter months, soil temperature was between 0 and −5 °C depending on the thickness of the snowpack and the timing of snowfall. Mean growing season volumetric soil water content (SWC) was 20.6 ± 1.1 %, dropping down to 14 % during the driest summer periods (Fig. 4b).

3.2.2. Seasonal CO_2 fluxes

Growing season mean daily NEE varied between −0.04 to 2.14 μmol m^{-2} s^{-1} at SLM (Fig. 4c). In 2020 and 2021, NEE showed a pronounced seasonal cycle driven by ecosystem respiration (ER), with high CO_2 emissions corresponding with periods of higher soil temperatures (Fig. 4c, e). However, in 2022, NEE fluctuated closer to zero during the growing season and the site recorded its first day with net mean CO_2 uptake in July, four years after the fire. Across all the measured years, ER closely followed the pattern of soil temperature (Fig. 4e). The seasonal amplitude of GPP increased every year after the fire, with daily means of up to 3.4 μmol m^{-2} s^{-1} by the fourth year after the fire (Fig. 4d).

3.2.3. Diurnal CO_2 fluxes

Net daytime CO_2 uptake at SLM started in 2022, the fourth growing season after the fire (Figs. 5a and 6a). At the beginning of June 2022, an abrupt increase in CO_2 uptake occurred and NEE then continued to be negative during the day throughout the growing season.

At the hourly scale, June-August NEE was similar during the night for all years and became increasingly more negative during the daytime with each year after the fire (Fig. 6a). In the second year after the fire (2020) NEE did not have a clear diurnal cycle and the site was a constant source of CO_2. In the following years, a clearer diurnal NEE pattern emerged, driven by GPP which had a much greater diurnal amplitude than ER during the main growing season.

3.2.4. Winter CO_2 fluxes

In 2022, we recorded the first dormant season (January-April, November-December) CO_2 fluxes at SLM (Fig. 4a). Although daily NEE was low (mean 0.21±0.10 μmol CO_2 m^{-2} s^{-1}) during these months, the sum of dormant season NEE (40 g C m^{-2} yr^{-1}) was equivalent to 13 % of the annual total CO_2 emissions (dormant season NEE + growing season ER).

3.2.5. Total carbon loss during and four years after the fire

During the second to fourth growing seasons post-fire, SLM was a net CO_2 source, with NEE growing season sums ranging between 113 and 202 g C m^{-2} (Fig. 7a). Growing season sums of ER and GPP increased every year since the fire. As GPP increased faster, there was a reduction in growing season C loss (decline in NEE) over time since the fire. In particular, GPP more than doubled in 2022 compared to 2021, suggesting a sharp increase in vegetation growth that summer. In total, 692 ± 13 g C m^{-2} of CO_2 was emitted since the fire at SLM during the growing season only (Fig. 7a, assuming that the 2019 sum of NEE was the same as in 2020), compared to 430 g C m^{-2} lost during the fire itself and 2200 g C m^{-2} removed from the site during the post-fire salvage-logging.

The model of annual NEE sums for the SLM site shows that it may take 13 years (8, 21; mean ± 95 % confidence intervals) after the fire until annual NEE at SLM reaches zero and the site starts to become a C sink again (model $R^2 = 0.66$, RMSE = 90 g C m^{-2} yr^{-1}; Fig. 7c). However, it could take 33 years (19, 54) after the fire to completely offset the C emitted during and after the fire (direct C loss + CO_2 emitted until NEE = 0). The latter estimate does not account for the large amount of C removed from the ecosystem during post-fire salvage-logging of the surviving trees. If the C removed by salvage-logging is also accounted

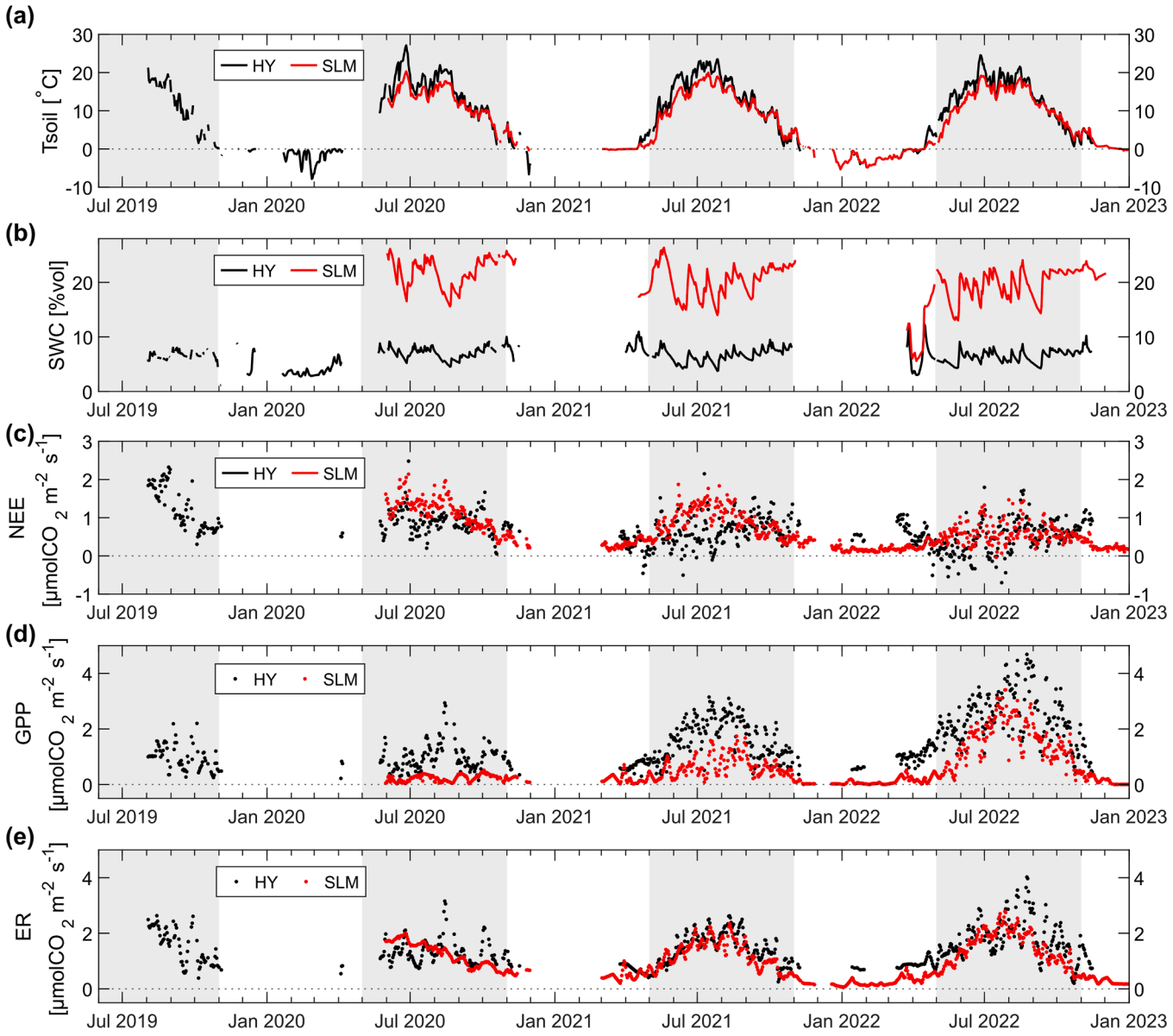

Fig. 4. Time series of mean daily soil temperature (Tsoil), soil water content (SWC) at 7.5 cm, NEE, GPP and ER. Shaded area depicts the growing season (1 May – 31 October). NEE, ER and GPP data are not shown for periods when NEE was gapfilled for >1 day in a row. SWC is not shown when the soil is completely frozen.

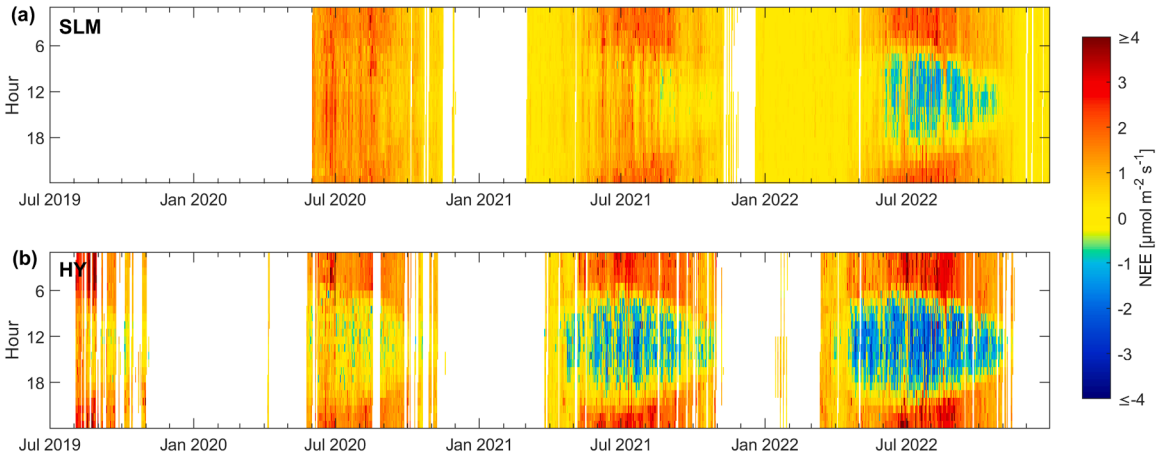

Fig. 5. Hourly averaged NEE at (a) SLM and (b) HY between July 2019 and December 2022. Data were discarded when NEE was gapfilled for >24 h consecutively.

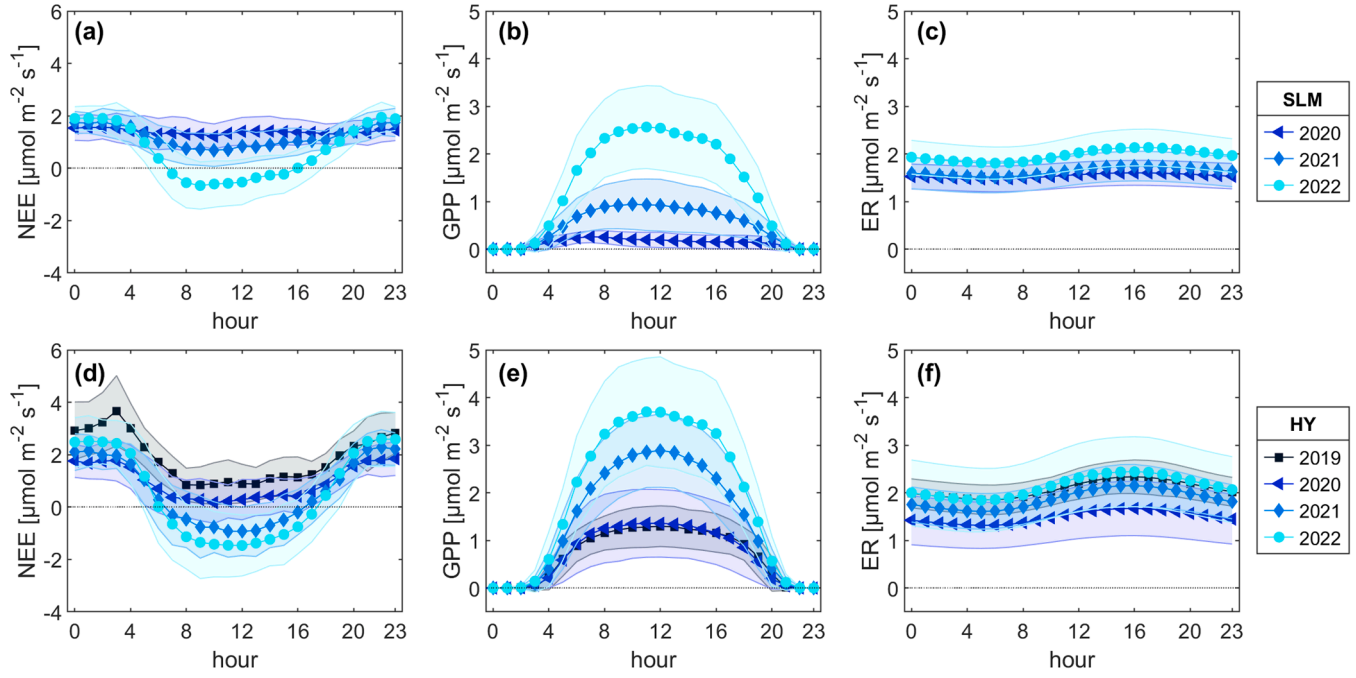

Fig. 6. Mean diurnal pattern of NEE, GPP and ER during June-August for SLM (a-c) and HY (d-f). Shaded areas represent ± 1σ.

for, it could take 46 years (31, 70) after the fire for all C lost to be offset. Our NEE estimates closely follow the NEE trajectory modelled by Coursolle et al. (2012) for Canadian boreal forests after disturbance (logging or wildfire) for the first four years after fire. However, the original Coursolle et al. (2012) model predicts smaller NEE in mature Canadian boreal forests compared to that predicted for mature, actively managed Swedish pine forests (Peichl et al. 2022a dataset).

3.2.6. *Vegetation recovery after the fire*

The Sentinel-2 EVI2 ($EVI2_{S2}$) dropped from 0.31 before the fire to ~0.1 in the first two years after the fire at SLM (Fig. 8a). Since then, $EVI2_{S2}$ has increased, although by 2022 it was only half of the level (0.15) observed at a nearby unburnt mature *Pinus sylvestris* stand (0.31). The longer MODIS time series shows stable $EVI2_{mod}$ at SLM for the four years preceding the fire. The in-situ measurements ($EVI2_{is}$) show a closer correspondence to the S2 than MODIS EVI2, which is expected, since the larger MODIS pixel size (250 m versus 10 m for S2) includes areas beyond the SLM flux tower footprint. The $EVI2_{is}$ data suggest a stronger increase in greenness from 2021 to 2022 compared to previous years, reflecting the same pattern seen in the growing season GPP sums (Fig. 7a).

The results of repeated vegetation surveys show that between 2020 and 2022, average vascular vegetation cover at SLM increased from 1.9 % to 2.8 % and bryophyte cover increased from 6.9 % to 28.9 %. In the 2022 survey, the most common vascular species was fireweed (*Chamaenerion angustifolium*), which was present in 58 % of the plots, followed by birch (*Betula sp*), with 17 % plot occupancy. *Polytrichum juniperum* was the most common bryophyte we surveyed (92 % plot occupancy). In the 2020 survey, we also recorded willow (*Salix* sp.) and European Aspen (*Populus tremula*) seedlings, and although they were not present in the quadrats in the 2022 survey, we did observe many seedlings at the site. The *Pinus sylvestris* seedling density was 1415 seedlings ha^{-1} at SLM in 2022, with an average height increase of 46 % (from 9 to 17 cm) between 2021 and 2022. It is not possible to estimate how many of these seedlings originate from the post-fire seed spreading versus natural regeneration.

3.3. *HY site*

3.3.1. *Soil conditions*

At the HY site, mean growing season soil temperature at 7.5 cm depth was 14.2 ± 0.9 °C but mean daily soil temperature often exceeded 20 °C during the summer and reached a maximum of 27 °C in June 2020, which was one of the warmest months of the entire study period (Figs. 3c and 4a). Volumetric soil water content (SWC) was generally <10 % as a result of the sandy mineral soil at the site, with a mean of 6.6 ± 0.3 % during the growing season (Fig. 4b).

3.3.2. *Seasonal CO_2 fluxes*

Growing season mean daily NEE varied between −0.70 to 2.48 µmol m^{-2} s^{-1} at HY (Fig. 4c). In 2019 and 2020, NEE followed the seasonal pattern of ER and GPP (Fig. 4a, c, e). A spike in GPP and ER during August 2020 may be an artefact of NEE gapfilling and partitioning because there were several consecutive days during this period when NEE had to be gapfilled, causing higher uncertainty in the partitioned fluxes. In 2021 and 2022, NEE fluctuated closer to 0 with the first days of net CO_2 uptake measured 3 years after the fire. High CO_2 emissions occurred in April and May 2022 as the soils began to thaw and the snowpack melted (Fig. 4c). Mean daily GPP increased with each year since the fire but even in the first growing season post-fire, there was evidence of CO_2 uptake (GPP maximum 2.2 µmol m^{-2} s^{-1}; Fig. 4d).

3.3.3. *Diurnal CO_2 fluxes*

At the hourly scale, HY had lower NEE during the day than at night during all measured growing seasons (Figs. 5b and 6d), highlighting the strong role of GPP in driving the daily NEE fluxes. Daytime CO_2 uptake has increased every year at HY, with the largest increase in 2021 relative to 2020 (i.e. the 3rd year after the fire, Fig. 6e). Even in the first growing season post-fire (2019), there was a notable GPP flux (~1 µmol m^{-2} s^{-1}, Fig. 6e). Nighttime NEE was also higher in 2019 than in the following growing seasons (Fig. 6d). We note that there were more gaps in the data during 2019 compared to the following years (Fig. 5b), increasing the uncertainty of our NEE and partitioned flux estimates in 2019.

Interestingly, measured and gapfilled nighttime NEE (Fig. 6d) are higher than modelled nighttime ER at HY in all years (Fig. 6c). This is partly due to the use of the daytime partitioning method, in which both

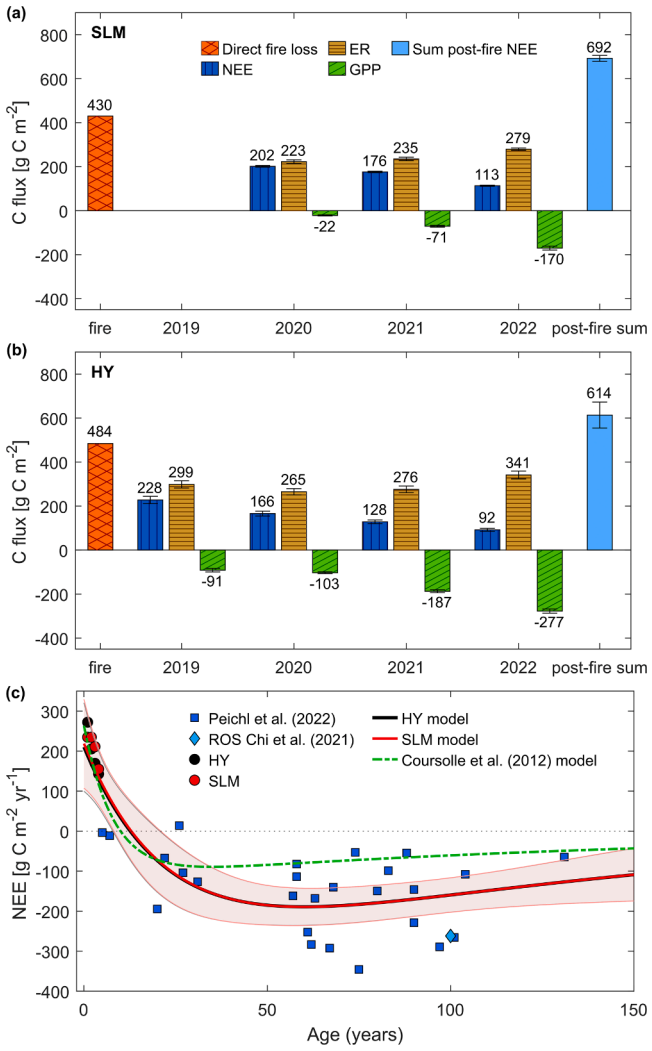

Fig. 7. Comparison of C lost during and after the fire at (a) SLM and (b) HY. NEE, ER and GPP bars represent the growing season sums of each flux based on our measurements. Due to the use of the daytime partitioning method, modelled estimates of GPP and ER do not sum up exactly to NEE. Error bars are standard deviation representing the uncertainty due to the choice of u* threshold and gapfilling. In 2019 at HY, measurements started in August, so we have doubled the August-October totals to estimate the growing season sum. In 2020 at both sites, measurements started in June, so the growing season sum is calculated as June-October sum + October sum. For the sum of post-fire NEE at SLM, we assumed that 2019 NEE was the same as in 2020. (c) Modelled NEE based on stand age combining data from this study, Peichl et al. (2022b) and Chi et al. (2021), and an NEE model for Canadian boreal forests from Coursolle et al. (2012). Shaded areas show 95 % confidence intervals for the modelled NEE, largely overlapping for the two sites.

GPP and ER are modelled and therefore nighttime ER does not always equal nighttime NEE (Wutzler et al., 2018). In addition, at HY, nighttime NEE had a higher proportion of missing data (compared to the daytime) which would lead to higher uncertainty in the temperature-sensitivity (E0) of the Lloyd and Taylor (1994) equation, which is estimated based on nighttime data (Wutzler et al., 2018).

3.3.4. Total carbon loss during and four years after the fire

In the first four growing seasons since the Ljusdal fire, HY has been a net CO_2 source, with NEE growing season sums ranging between 92 and 228 g C m^{-2} (Fig. 7b). GPP has increased every year since the fire, leading to declining NEE growing season sums (i.e. lower C emission). During the first four years since the fire, 614 ± 59 g C m^{-2} was emitted

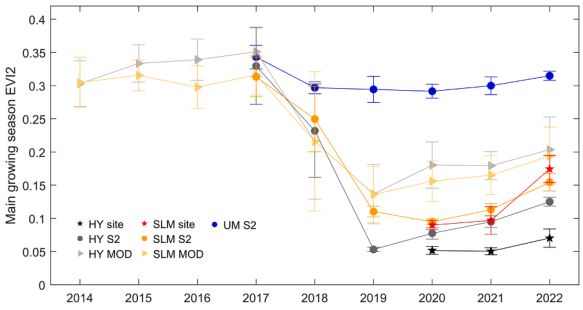

Fig. 8. Time series with average June-August EVI2 from in-situ sensors ('site', $EVI2_{is}$), Sentinel-2 ('S2', $EVI2_{S2}$) and MODIS ('MOD', $EVI2_{mod}$). $EVI2_{S2}$ and $EVI2_{mod}$ are the footprint weighted average of all pixels within the flux-tower footprint. Blue circles show $EVI2_{S2}$ from an unburnt mature (UM) *Pinus sylvestris* stand within 3 km of the HY and SLM sites. Error bars are ± σ and account for the temporal range of EVI2.

at HY during the growing season only, compared to 484 g C m^{-2} lost from combustion during the fire (Fig. 7b). The modelled recovery of NEE since the fire at HY was almost identical to that for SLM (Fig. 7c). The model predicted that the source to sink transition (where annual NEE becomes 0) would occur within 13 years (8, 21; mean ± 95 % confidence intervals) of the fire at HY whilst it could take 32 years (19, 53) for C losses during and after the fire to be offset by C uptake at HY.

3.3.5. Vegetation recovery after the fire

The MODIS time series shows that site greenness was increasing at HY in the 4 years before the fire, as expected for such a young forest (Fig. 8a). Similarly to SLM, the $EVI2_{mod}$ at HY was higher compared to $EVI2_{S2}$ and $EVI2_{is}$, likely due to mixed pixels in the MODIS data. The $EVI2_{S2}$ for HY was lowest in 2019, the year after the fire, and has increased linearly since then (from 0.05 to 0.13). The $EVI2_{is}$ measurements suggest a slower rate of recovery compared to the $EVI2_{S2}$ data. Due to the patchiness of the vegetation regrowth at HY, the $EVI2_{is}$ sensor at HY may not fully capture the vegetation dynamics across the whole site, although it does capture vegetation regrowth in the area nearest the EC tower which has the largest impact on the flux measurements.

At HY, between 2020 and 2022, vascular vegetation cover increased from <1 % to 4.4 % whereas bryophyte cover jumped from 1.8 % to 27 %. The most common species was *Polytrichum juniperum* which appeared in all but one quadrat in 2022, followed by *Chamaenerion angustifolium* (in 42 % of quadrats) and *Calluna vulgaris* (16 % quadrat occupancy). The only tree species recorded were *Pinus sylvestris* and *Betula* sp. The pine seedling density in 2022 was 2299 seedlings ha^{-1}, and the average height of the seedlings more than doubled between 2021 and 2022 from 24 to 52 cm.

4. Discussion

4.1. Carbon budget in the early post-fire years

As access to recently burnt forests is often restricted, very few previous studies have been able to capture a time series of flux measurements during the initial years after a forest fire, when the largest C emissions are expected. We found that *Pinus sylvestris* stands burnt at high- or low-severity were net CO_2 sources during the first four years post-fire. Given that hardly any vegetation remained after the fire and/or salvage-logging, it is not surprising that our sites were net CO_2 sources. Our growing season NEE sums of 128–176 g C m^{-2} in 2021 are in line with a measured net emission of 132 g C m^{-2} during the third year after a stand-replacing fire in a Canadian boreal forest (Amiro et al., 2006). The total net C emitted during the first three years after the Ljusdal fire, between 647 and 681 g C m^{-2}, was a third higher than the ~440 g C m^{-2} emitted during the first 3 years after a stand-replacing fire

in a *Pinus sylvestris* forest in central Sweden (Granath et al., 2020) . The difference between the estimates may be due to faster vegetation recovery at the site studied by Granath et al., which is further south, and/or uncertainties in the estimates of C loss from the first year post-fire, which were partly modelled in both studies. The 2021 growing season C loss estimate from SLM (176 g C m^{-2}) is within the range observed at other boreal sites in Sweden and Canada 3 years after clear-cut (no fire; 123–443 g C m^{-2} yr^{-1}; Mkhabela et al. (2009); Vestin et al. (2020).

4.1.1. Reduction in ecosystem respiration after fire

Although our sites were net C sources after the fire, ER was lower than at undisturbed pine sites. The growing season sums of ER we measured were only 45–68 % of the ER of an unburnt mature *Pinus sylvestris* stand in northern Sweden with similar soil type (ER = 500 g C m^2 at Rosinedalsheden; Chi et al., 2021). Other boreal fire studies have also found lower soil or ecosystem respiration after fire compared to unburnt sites, with the lowest rates at the youngest burnt sites and after high severity fire (Amiro et al., 2003; Goulden et al., 2011; Gui et al., 2023). Note that both our sites had similarly low ER after the fire, despite experiencing different fire severities. This is most likely due to the salvage-logging of the surviving trees at SLM. If the trees at SLM had not been salvage-logged, we would have expected the soil respiration to be higher and similar to that of an unburnt forest, based on previous chamber flux measurements in our study area (Kelly et al., 2021). The salvage-logging of living trees seems to imitate the effects of a high severity fire on ER, implying that vegetation mortality is a key driver of post-fire respiration. These findings are reflected in previous studies of boreal fires which have shown that post-fire ER is mainly driven by autotrophic respiration as vegetation re-establishes (Czimczik et al., 2006; Goulden et al., 2011; Singh et al., 2008).

Vegetation mortality not only reduces autotrophic respiration but also the heterotrophic respiration of symbiotic soil microbes. Higher tree mortality has been linked to higher losses of soil microbial biomass after Swedish forest fires (Eckdahl et al. 2023). The loss of living trees at both our sites would have significantly reduced the inputs of labile C substrates from photosynthesis that microbial groups such as ectomycorrhizal fungi, a key group in boreal forests, depend on (Pérez-Izquierdo et al., 2020). In addition, the death of soil microbes due to the consumption of the soil organic layer during a fire can further reduce heterotrophic respiration and thus ER post-fire (Certini et al., 2021).

Both our sites have some coarse woody debris left behind by the fire and/or salvage-logging but it is unclear how much this may have contributed to ER. At SLM, the roots of the dead trees remained in the soil and tree branches were left on site. At HY, the thin dead trees remained standing after the fire but are increasingly falling down. Martínez-García et al. (2017) have shown that burnt tree stumps can be hot spots of soil respiration 1–4 years after fire in Spanish pine forests. However, others have shown that respiration fluxes are highest in more decayed burnt wood and emphasized that it takes decades for coarse woody or charcoaled debris to fully decompose (Bond-Lamberty et al., 2002; Goulden et al., 2011; Yatskov et al., 2003).

4.1.2. Recovery of CO_2 uptake

Surprisingly, HY already showed a notable reduction in daytime NEE during the first growing season after fire. Drone imagery collected that year and photos from the site confirm that patches of fireweed (*Chamaenerion angustifolium*) were starting to colonize HY. Fireweed grows rapidly, and is the most common early pioneer species after fire in Sweden (Gustafsson et al., 2020). It also helped drive CO_2 uptake after fire in the Canadian boreal forest (Goulden et al., 2006). Both our sites recorded their first day of net CO_2 uptake within four years after the fire, similar to results in post-fire Canadian forests (Amiro et al., 2003; Goulden et al., 2006). The $EVI2_{S2}$ data indicated increased vegetation coverage with time since the fire. At both our sites, the reduction in NEE during the first four years since the fire was driven by the more rapid increase of GPP compared to ER as vegetation has established. The same trend was identified by Amiro et al. (2003) with EC measurements from the first decade after Canadian boreal forest fires.

4.2. Impact of post-fire forest management on the carbon balance

Our sites experienced two different strategies for post-fire management: planting of pine seedlings (HY) and salvage-logging of surviving trees followed by soil scarification and spreading of pine seeds (SLM). There are no statistics available on how common these different types of management approaches are after fire but they are part of standard Swedish forestry practices and advice given to forest owners after the Ljusdal fire (Skogsstyrelsen, 2018). The fact that living trees were salvage-logged, turning SLM into a net C source, highlights the need for research evaluating the environmental, economic and societal costs and benefits of post-fire forest management decisions.

Both sites are recovering from the fire at a similar pace, in terms of NEE and vegetation cover, but the recovery is driven by different vegetation species which partly results from the choice of post-fire forest management method. At HY, the pine seedlings have shown vigorous growth and their density is 60 % higher at HY than SLM. Thus at HY, the increasing GPP is likely driven mainly by the replanted seedlings, as well as the high abundance of fireweed. At SLM however, recovery of GPP is driven by deciduous tree seedlings such as willow, birch and European aspen that are outcompeting the reseeded pine. The failed germination of the pine seeds at SLM may be due to freeze-thaw pushing them out of the scarified soil (Skogsstyrelsen, 2018). The fact that pine seedlings were planted at HY may have been critical to them being able to survive the harsh soil microclimate at HY compared to if seeds had been spread. The difference in the seasonal pattern of NEE at the two sites (Fig. 5) confirms these differences in the dominant vegetation type. At SLM, in 2022, the abrupt start of CO_2 uptake in June likely coincides with leaf-out in the deciduous tree seedlings. In contrast, HY has a longer period of net CO_2 uptake than at SLM since the coniferous pine seedlings planted at HY can begin photosynthesizing as soon as the snow melts in spring and can continue during warm autumn days, after the senescence of the deciduous vegetation at SLM. In the long-term, *Pinus sylvestris* abundance will likely increase at SLM because it is well-adapted to the dry, shallow soils found in these regions (Gustafsson et al., 2020). Within 5–10 years after the salvage-logging, the deciduous trees are likely to be removed as part of standard management practices to promote the growth of commercial pine.

4.3. Long-term recovery of the carbon balance

We predicted that it could take on average 13 years after the fire until both sites are net neutral at the annual scale, but over three decades for all C lost during and after the fire to have been completely offset by post-fire C uptake at both sites (i.e. to reach the C compensation point). It would take more than four decades if accounting for the C removed during the post-fire salvage-logging at SLM. These estimates of recovery time are uncertain, in part due to the simple calculation we used to transform measured growing season NEE into annual NEE sums, the lack of available dormant season flux measurements at HY and the missing NEE data from the first year after the fire at SLM. The uncertainty is reflected in the 95 % confidence intervals of the models, which, for example, indicated that annual C neutrality could be reached within 8–21 years (mean 13 years) post-fire at both sites. The model also assumes that the change in NEE with tree age at our wildfire-affected sites will be similar to that from the unburnt sites in Peichl et al. 2022b and Chi et al. (2021). This assumption is justified since the time taken until disturbed boreal forests reach NEE = 0 at the annual scale is similar for unburnt, clear-cut forest sites in southern Sweden (8–13 years) and burnt boreal forest sites in Canada (10–18 years) and Alaska (13 years; (Coursolle et al., 2012; Grelle et al., 2023; Ueyama et al., 2019). Our mean modelled estimates of the time needed to reach the C

compensation point (32–46 years) are notably longer than the 18 years needed to reach the C compensation point in northern Swedish forests after clear-cutting (Peichl et al., 2022b). Although there is significant uncertainty in these estimates (95 % confidence intervals 19–53 years at HY and 31–70 years at SLM), they nevertheless highlight the potentially long-lasting effects of the fire and salvage-logging.

4.4. Relative carbon losses during and after fire

There are very few in-situ measurements comparing the relative importance of C emissions during and after fire in boreal forests. Studies of forest fires in Sweden and Alaska have shown that the cumulative post-fire C emissions during the first 3–13 years after fire only account for up to a third of the C lost during a fire (Granath et al., 2021; Ueyama et al., 2019). At our sites however, C emissions from the first four growing seasons after fire (mean of both sites 653 g C m^{-2}) were higher than the direct fire C emissions (mean of both sites 457 g C m^{-2}). There is some uncertainty in the absolute value of direct fire C loss at SLM because the estimate is based on data from a nearby, similar low-severity fire site. Nevertheless, our post-fire C loss estimates are within the range of direct fire C losses from 50 low to moderate severity forest fires that occurred across Sweden in 2018 (mean 815±625 g C m^{-2} Eckdahl et al. (2022). Our results therefore underline the importance of C emissions during the initial years after fire when calculating the net impact of fire on the C budget of managed boreal forests. Only including the CO_2 fluxes should account for the vast majority of the C lost since the fire because measurements of soil CH_4 fluxes from the study area show a negligible CH_4 uptake (Kelly et al., 2021) and loss of C via leaching is likely to be minimal (Granath et al., 2021)

Our estimates of direct C loss from the fire are low compared to C combustion from fires in Siberian pine and larch forests (1.69–3.36 kg C m^{-2}; Veraverbeke et al. (2021) and those in Canadian jack pine and black spruce forests (1.3–3.6 kg C m^{-2}; Dieleman et al. (2020); Santín et al. (2015), and very low compared to the 2014 Västmanland fire in central Sweden (4.5 kg C m^{-2}; Granath et al. (2021). Our C combustion estimates are lower because of the combination of our site and fire characteristics. The forests in our study area only have a thin forest floor layer which is underlain by shallow, nutrient-poor sandy soils, which reduced C emissions during fire compared to the C emissions from boreal forests on peat or deep organic soil layers, such as those affected by the Västmanland fire (Granath et al., 2021). Furthermore, SLM experienced low-severity ground fire, which is common across Eurasia but contrasts with the stand-replacing fires of boreal North America that tend to have higher C emission rates and higher combustion of soil C (De Groot et al., 2013; Veraverbeke et al., 2021). At HY, on the other hand, the trees were only 10 years old at the time of the fire, leaving little time for forest floor C and vegetation biomass to accumulate since the previous clear-cut. Monitoring the C budget of stands like HY which have been affected by multiple disturbances before the stand can fully recover (in this case clear-cutting followed by fire 10 years later) is critical because disturbance frequency and land use change are intensifying. As a result, forests around the world are becoming younger (McDowell et al., 2020). Our findings highlight the significance of monitoring post-fire recovery in the managed forests of the Nordic countries, where low-severity fire, multiple disturbances (fire and logging) and a thin forest floor layer can combine to increase the importance of emissions after fire relative to the direct emissions from combustion.

5. Conclusions

Although fire suppression has been highly successful in Sweden for over a century, the high number of forest fires in 2018 highlighted the vulnerability of these forests to future summer droughts and extreme fire seasons that could overwhelm available firefighting resources. The fierce debate around the carbon sequestration potential, as well as the economic significance, of Sweden's intensively managed forests emphasizes the importance of studies assessing how disturbances impact these forests. We have presented the first detailed assessment of CO_2 fluxes after forest fire in the Nordic boreal forest and helped fill the gap in measurements of forest carbon (C) fluxes during the early years after a fire. Both our *Pinus sylvestris* sites were net carbon sources for the first four growing seasons after the fire, and we predict that it will take at least a decade before they become carbon neutral at the annual scale, and over three decades before the cumulative fire and post-fire C losses are fully recovered. We have shown that in young stands affected by high-severity fire and in mature stands affected by low-severity fire with subsequent salvage-logging, post-fire carbon losses can outweigh direct fire carbon emissions within the first four years after fire. Our results provide a crucial benchmark for modellers seeking to predict the effects of low-severity fires and fires in managed boreal forests. While management decisions related to salvage-logging had a large impact on post-fire C loss, decisions on how to replant stands had less of an impact on the carbon balance of recovering sites during the first few years after fire. Ongoing research in the Ljusdal fire area will further disentangle the effect of management and fire severity on ecosystem and soil carbon fluxes, nutrient cycling and microbial recovery since the fire.

CRediT authorship contribution statement

Julia Kelly: Writing – review & editing, Writing – original draft, Visualization, Investigation, Funding acquisition, Formal analysis, Data curation. **Natascha Kljun:** Writing – review & editing, Supervision, Resources, Project administration, Methodology, Investigation, Funding acquisition, Data curation, Conceptualization. **Zhanzhang Cai:** Software. **Stefan H. Doerr:** Writing – review & editing, Resources, Methodology, Investigation, Funding acquisition, Conceptualization. **Claudio D'Onofrio:** Software, Methodology, Investigation, Data curation. **Thomas Holst:** Writing – review & editing, Resources, Methodology, Investigation, Funding acquisition. **Irene Lehner:** Software, Investigation, Data curation. **Anders Lindroth:** Writing – review & editing, Resources, Methodology, Funding acquisition, Conceptualization. **Shangharsha Thapa:** Software, Formal analysis. **Patrik Vestin:** Methodology. **Cristina Santín:** Writing – review & editing, Resources, Methodology, Investigation, Funding acquisition, Conceptualization.

Declaration of competing interest

The authors declare that they have no known competing financial interests or personal relationships that could have appeared to influence the work reported in this paper.

Data availability

Data will be made available on zenodo and FLUXNET

Acknowledgements

This research was funded by FORMAS grants #2018–02700 and 2019–00836, the Crafoord foundation grant 20190763, Skogssällskapet Stina Werner Fond grant 2021–094 and the Royal Physiographic Society of Lund. It is a contribution to the Strategic Research Areas MERGE (ModElling the Regional and Global Earth system) and BECC (Biodiversity and Ecosystem Services in a Changing Climate), funded by the Swedish government. We thank David Allbrand and Leif Klemedtsson for their help with the SLM tower and Marco Hassoldt for his ongoing support. Thanks also to Rolf Sundell and the other forest owners for allowing us to conduct research on their land and to Jukka Kuivaniemi for helping us establish the sites. We are grateful to Gabriel Gosselin and Alexander Graf for providing us with the codes to run the Papale filter and the roughness length derivations.

Supplementary materials

Supplementary material associated with this article can be found, in the online version, at doi:10.1016/j.agrformet.2024.110016.

References

Amiro, B.D., 2001. Paired-tower measurements of carbon and energy fluxes following disturbance in the boreal forest. Glob. Chang. Biol. 7 (3), 253–268.

Amiro, B.D., et al., 2006. Carbon, energy and water fluxes at mature and disturbed forest sites, Saskatchewan, Canada. Agric. For. Meteorol. 136 (3-4), 237–251.

Amiro, B.D., Macpherson, J.I., Desjardins, R.L., Chen, J.M., Liu, J., 2003. Post-fire carbon dioxide fluxes in the western Canadian boreal forest: evidence from towers, aircraft and remote sensing. Agric. For. Meteorol. 115, 91–107.

Anderegg, W.R.L., et al., 2022. A climate risk analysis of Earth's forests in the 21st century. Science (1979) 377 (6610), 1099–1103.

Bansal, S., Jochum, T., Wardle, D.A., Nilsson, M.C., 2014. The interactive effects of surface-burn severity and canopy cover on conifer and broadleaf tree seedling ecophysiology. Canadian Journal of Forest Research 44 (9), 1032–1041.

Bond-Lamberty, B., Peckham, S.D., Ahl, D.E., Gower, S.T., 2007. Fire as the dominant driver of central Canadian boreal forest carbon balance. Nature 450 (7166), 89–92.

Bond-Lamberty, B., Wang, C., Gower, S.T., 2002. Annual carbon flux from woody debris for a boreal black spruce fire chronosequence. Journal of Geophysical Research: Atmospheres 107 (D23). WFX 1-1-WFX 1-10.

Certini, G., Moya, D., Lucas-Borja, M.E., Mastrolonardo, G., 2021. The impact of fire on soil-dwelling biota: A review. For. Ecol. Manage 488.

Chi, J., et al., 2021. Forest floor fluxes drive differences in the carbon balance of contrasting boreal forest stands. Agric. For. Meteorol. 306.

CLMS, 2023. High Resolution Vegetation Phenology and Productivity (HRVPP): seasonal trajectories, vegetation phenology and productivity paramaters.

Coursolle, C., et al., 2012. Influence of stand age on the magnitude and seasonality of carbon fluxes in Canadian forests. Agric. For. Meteorol. 165, 136–148.

Czimczik, C.I., Trumbore, S.E., Carbone, M.S., Winston, G.C., 2006. Changing sources of soil respiration with time since fire in a boreal forest. Glob. Chang. Biol. 12 (6), 957–971.

De Groot, W.J., et al., 2013. A comparison of Canadian and Russian boreal forest fire regimes. For. Ecol. Manage 294, 23–34.

Dieleman, C.M., et al., 2020. Wildfire combustion and carbon stocks in the southern Canadian boreal forest: Implications for a warming world. Glob. Chang. Biol. 26 (11), 6062–6079.

Dooley, S.R., Treseder, K.K., 2012. The effect of fire on microbial biomass: a meta-analysis of field studies. Biogeochemistry. 109 (1/3), 49–61.

Eckdahl, J.A., Kristensen, J.A., Metcalfe, D.B., 2022. Climatic variation drives loss and restructuring of carbon and nitrogen in boreal forest wildfire. Biogeosciences. 19, 2487–2506.

Feurdean, A., et al., 2020. Recent fire regime in the southern boreal forests of western Siberia is unprecedented in the last five millennia. Quat. Sci. Rev. 244.

Gauthier, S., Bernier, P., Kuuluvainen, T., Shvidenko, A.Z., Schepaschenko, D.G., 2015. Boreal forest health and global change. Science (1979) 349 (6250), 819–822.

Goulden, M.L., et al., 2011. Patterns of NPP, GPP, respiration, and NEP during boreal forest succession. Glob. Chang. Biol. 17, 855–871.

Goulden, M.L., et al., 2006. An eddy covariance mesonet to measure the effect of forest age on land-atmosphere exchange. Glob. Chang. Biol. 12 (11), 2146–2162.

Graf, A., et al., 2014. Intercomparison of methods for the simultaneous estimation of Zero-Plane displacement and aerodynamic roughness length from Single-Level Eddy-Covariance data. Boundary-Layer Meteorol. 151, 373–387.

Granath, G., et al., 2021. The impact of wildfire on biogeochemical fluxes and water quality on boreal catchments. Biogeosciences. 18, 3243–3261.

Grelle, A., Hedwall, P.O., Strömgren, M., Håkansson, C., Bergh, J., 2023. From source to sink – recovery of the carbon balance in young forests. Agric. For. Meteorol. 330.

Gui, H., Wang, J., Hu, M., Zhou, Z., Wan, S., 2023. Impacts of fire on soil respiration and its components: A global meta-analysis. Agric. For. Meteorol. 336.

Gustafsson, L., Granath, G., Nohrstedt, H.Ö., Leverkus, A.B., Johansson, V., 2020. Burn severity and soil chemistry are weak drivers of early vegetation succession following a boreal mega-fire in a production forest landscape. Journal of Vegetation Science 0–3.

Houghton, R.A., Hall, F., Goetz, S.J., 2009. Importance of biomass in the global carbon cycle. Journal of Geophysical Research: Biogeosciences 114 (G2) n/a-n/a.

Högberg, P., et al., 2021. Sustainable Boreal Forest management: Challenges and Opportunities For Climate Change Mitigation, 11. Skogsstyrelsen.

IPCC, 2023. Summary for Policymakers. In: Team, C.W., Lee, H., Romero, J. (Eds.), Climate Change 2023: Synthesis Report. A Report of the Intergovernmental Panel on Climate Change. Contribution of Working Groups I, II and III to the Sixth Assessment Report of the Intergovernmental Panel on Climate Change. Geneva, Switzerland. IPCC, p. 36.

Jarvis, P., Linder, S., 2000. Constraints to growth of boreal forests. Nature 405, 904–905.

Jiang, Z., Huete, A.R., Didan, K., Miura, T., 2008. Development of a two-band enhanced vegetation index without a blue band. Remote Sens. Environ. 112 (10), 3833–3845.

Jönsson, P., Eklundh, L., 2004. TIMESAT - A program for analyzing time-series of satellite sensor data. Computers and Geosciences 30 (8), 833–845.

Kelly, J., et al., 2021. Boreal forest soil carbon fluxes one year after a wildfire: Effects of burn severity and management. Glob. Chang. Biol. 27 (17), 4181–4195.

Kelly, R., et al., 2013. Recent burning of boreal forests exceeds fire regime limits of the past 10,000 years. Proc. Natl. Acad. Sci. u S. a 110 (32), 13055–13060.

Kljun, N., Calanca, P., Rotach, M.W., Schmid, H.P., 2015. A simple two-dimensional parameterisation for Flux Footprint Prediction (FFP). Geosci. Model. Dev. 8 (11), 3695–3713.

Lasslop, G., et al., 2010. Separation of net ecosystem exchange into assimilation and respiration using a light response curve approach: Critical issues and global evaluation. Glob. Chang. Biol. 16 (1), 187–208.

Litvak, M., Miller, S., Wofsy, S.C., Goulden, M., 2003. Effect of stand age on whole ecosystem CO2 exchange in the Canadian boreal forest. Journal of Geophysical Research: Atmospheres 108 (3), 1–11.

Lloyd, J., Taylor, J.A., 1994. On the Temperature Dependence of Soil Respiration. Funct. Ecol. 8 (3), 315-315.

Mack, M.C., et al., 2021. Carbon loss from boreal forest wildfires offset by increased dominance of deciduous trees. Science (1979) 372, 280–283.

Marklund, L.G., 1988. Biomass Functions For pine, Spruce and Birchin Sweden, 45. Department of Forest Survey, Umeå.

Martínez-García, E., et al., 2017. Medium-term dynamics of soil respiration in a Mediterranean mountain ecosystem: The effects of burn severity, post-fire burnt-wood management, and slope-aspect. Agric. For. Meteorol. 233, 195–208.

McDowell, N.G., et al., 2020. Pervasive shifts in forest dynamics in a changing world. Science (1979) 368 (6494) eaaz9463-eaaz9463.

Meyers, T., 2004. An assessment of storage terms in the surface energy balance of maize and soybean. Agric. For. Meteorol. 125 (1-2), 105–115.

Mkhabela, M.S., et al., 2009. Comparison of carbon dynamics and water use efficiency following fire and harvesting in Canadian boreal forests. Agric. For. Meteorol. 149 (5), 783–794.

Peichl, M., et al., 2022a. Data Set For "Landscape-variability of the Carbon Balance Across Managed Boreal Forests. Zenodo.

Peichl, M., et al., 2022b. Landscape-variability of the carbon balance across managed boreal forests. Glob. Chang. Biol.

Pérez-Izquierdo, L., et al., 2020. Crown-fire severity is more important than ground-fire severity in determining soil fungal community development in the boreal forest. Journal of Ecology 1–15.

Santín, C., Doerr, S.H., Preston, C.M., González-Rodríguez, G., 2015. Pyrogenic organic matter production from wildfires: a missing sink in the global carbon cycle. Glob. Chang. Biol. 21 (4), 1621–1633.

Singh, S., Amiro, B.D., Quideau, S.A., 2008. Effects of forest floor organic layer and root biomass on soil respiration following boreal forest fire. Canadian Journal of Forest Research 38 (4), 647–655.

SITES, 2022. SITES Spectral - Data Quality Flagging (QFLAG) Documentation. SITES Spectral.

Skogsstyrelsen, 2018. Skogsbränderna 2018 i Dalarna, Hälsingland, Härjedalen och Jämtland: Föryngringsmetoder för brandfälten. Skogsstyrelsen.

SMHI, 2023. Ytterhogdal. In: SMHI (Editor). SMHI, pp. Meteorological data.

Trivino, M., et al., 2022. Future supply of boreal forest ecosystem services is driven by management rather than by climate change. Glob. Chang. Biol.

Ueyama, M., et al., 2019. Carbon dioxide balance in early-successional forests after forest fires in interior Alaska. Agric. For. Meteorol. 275 (November 2018), 196–207.

Veraverbeke, S., et al., 2021. Direct and longer-term carbon emissions from arctic-boreal fires: A short review of recent advances. Curr. Opin. Environ. Sci. Health 23.

Vestin, P., et al., 2020. Impacts of Clear-Cutting of a Boreal Forest on Carbon Dioxide, Methane and Nitrous Oxide Fluxes. Forests. 11 (961), 1–28.

Walker, X.J., et al., 2019. Increasing wildfires threaten historic carbon sink of boreal forest soils. Nature 572 (7770), 520–523.

Wilhelmsson, L., et al., 2002. Models for predicting wood properties in stems of Picea abies and Pinus sylvestris in Sweden. Scandinavian Journal of Forest Research 17 (4), 330–350.

Wutzler, T., et al., 2018. Basic and extensible post-processing of eddy covariance flux data with REddyProc. Biogeosciences. 15 (16), 5015–5030.

Yatskov, M., Harmon, M.E., Krankina, O.N., 2003. A chronosequence of wood decomposition in the boreal forests of Russia. Canadian Journal of Forest Research 33 (7), 1211–1226.